Journal of Physics: Conference Series **436** (2013) 012033 doi:10.1088/1742-6596/436/1/012033

The geometric interpretation of the semimicroscopic algebraic cluster model and the role of the Pauli principle

H Yépez-Martínez[1], P O Hess[2,3,4] and G Lévai[5]

[1]Universidad Autónoma de la Ciudad de México, Prolongación San Isidro 151, Col. San Lorenzo Tezonco, Del. Iztapalapa, 09790 México D.F., Mexico
[2] Instituto de Ciencias Nucleares, UNAM, Circuito Exterior, C.U., A.P. 70-543, 04510 México, D.F., Mexico
[3] Frankfurt Institute for Advanced Studies (FIAS), J.W. von Goethe Universität, Ruth-Moufang-Str. 1, 60438 Frankfurt am Main, Germany
[4] GSI für Schwerionenforschung Helmholzzentrum GmbH,Max-Planck-Str. 1 64291 Darmstadt, Germany
[5]Institute of Nuclear Research of the Hungarian Academy of Sciences, Debrecen, Pf. 51, Hungary-4001

E-mail: hess@nucleares.unam.mx

Abstract. We study the properties of the Semimicroscopic Algebraic Cluster Model (SACM) under phase transitions. We show that the SACM can undergo first and second order phase transitions and a critical line appears. When the Pauli principle is not observed, the critical line appears, but other non-physical properties arise. At the end the meaning of the $SO(4)$ dynamical limit is discussed.

1. Introduction

In this contribution the structure of phase transition within the SACM is discussed. The same will be done when the Pauli exclusion principle is not taken into account. Some physical interpretation of the $SO(4)$ limit is also given. The discussion of phase transitions is enormously simplified when a geometrical mapping is applied. A semi-classical potential is obtained which depends on variables related to physical observables as the distance between two clusters. Phase transitions then manifest themselves by certain structural changes in the potential.

In section 2 the SACM is shortly reviewed, the Hamiltonian is defined and the method of geometrical mapping is explained. The semi-classical potential is obtained, which is used to investigate the phase transitions of the model. Changes are discussed when the Pauli exclusion principle is not observed. At the end some remarks are made concerning the physical meaning of the $SO(4)$ dynamical limit. In section 3 conclusions are drawn.

2. The SACM and the geometrical mapping

We shall shortly resume the main features of the SACM [1, 2]. The relative degrees of freedom are described by the oscillator boson operators $\pi^\dagger_m$ and π_m, with $m = 0, \pm 1$. To that the scalar boson operators $\sigma^\dagger$ and σ are also added: these have no physical meaning but are needed in

order to introduce a cutoff in the theory. All combinations of any creation with any annihilation operator form the $U_R(4)$ group, where the R refers to the relative motion. The total number of bosons $N = n_\pi + n_\sigma$ is kept constant, i.e., the number of π-bosons ranges from 0 to N. The individual clusters are described via the $SU(3)$-model of Elliott [3]. In this way both the relative motion and the orbital structure of the clusters is characterized by an $SU(3)$ irreducible representation (irrep) (λ, μ).

The model space is constructed as follows. First, one determines the result of the product $(\lambda_1, \mu_1) \otimes (\lambda_2, \mu_2) \otimes (n_\pi, 0)$, which gives a sum of total $SU(3)$ irreps with a certain multiplicity. Second, all possible excitations of the nucleons within the shell model are constructed, for $n\hbar\omega$ excitation, with the center of mass removed. This list of shell model irreps, which by construction observe the Pauli exclusion principle is compared to the former list. Only those irreps are included in the SACM model space, which appear also in the shell model space. This method automatically reproduces the Wildermuth condition, which states that there is a minimal number of π-bosons (n_0) needed as a necessary condition to satisfy the Pauli exclusion principle. In this manner, the Pauli exclusion principle is observed. Since the model space is constructed microscopically, one can study in this framework the overlap of the cluster configurations with the states of the shell and collective models, e.g. the clusterization of the superdeformed (SD) and hyperdeformed (HD) states. It is remarkable that the predictions of the model seem to be justified by the experimental observation in some cases, like for the SD state of ^{28}Si [4] and for the HD state of the ^{36}Ar [5].

The Hamiltonian is phenomenological, indicated by "semi" in the acronym SACM. We consider the sum of Hamiltonians, each describing a particular dynamical symmetry limit. Due to lack of space we shall present here the Hamiltonian taking into account only the $SU(3)$ and $SO(4)$ dynamical symmetries. The first one is known as the *vibrational limit*, while the second one as the *deformed limit*, though, as will be shown below, within the SACM the potential is already deformed by construction.

The Hamiltonian has the form

$$\boldsymbol{H} = x\boldsymbol{H}_{SU(3)} + (1-x)\boldsymbol{H}_{SO(4)} \ , \tag{1}$$

where x is the parameter ranging from 0 to 1, determining the relative weight of each symmetry. In their most general form, the individual components are

$$\begin{aligned}
\boldsymbol{H}_{SU(3)} &= \hbar\omega\boldsymbol{n}_\pi + a_C\boldsymbol{C}_2(\lambda_C,\mu_C) + (\bar{a} - \bar{b}\triangle\boldsymbol{n}_\pi)\boldsymbol{C}_2\,(n_\pi,0) + (a - b\triangle\boldsymbol{n}_\pi)\,\boldsymbol{C}_2(\lambda,\mu) + \gamma\boldsymbol{L}^2 + t\boldsymbol{K}^2 \\
\boldsymbol{H}_{SO(4)} &= a_C\boldsymbol{C}_2(\lambda_C,\mu_C) + a_C{\boldsymbol{L}_C}^2 + a_R^{(1)}{\boldsymbol{L}_R}^2 + \gamma\boldsymbol{L}^2 + \frac{c}{4}\left[\left(\boldsymbol{\pi}^\dagger\cdot\boldsymbol{\pi}^\dagger\right) - \left(\boldsymbol{\sigma}^\dagger\right)^2\right]\left[(\boldsymbol{\pi}\cdot\boldsymbol{\pi}) - (\boldsymbol{\sigma})^2\right] \ .
\end{aligned} \tag{2}$$

The $SU(3)$ Hamiltonian contains a third-order interaction. Because the interaction proportional, for example, to the $\boldsymbol{C}_2(n_\pi, 0)$ interaction is given by $\boldsymbol{n}_\pi(\boldsymbol{n}_\pi + 3)$, this term dominates for large n_π and destroys the mean field part $\hbar\omega\boldsymbol{n}_\pi$. In models with a fixed number of n_π this is avoided by limiting the model space to few $\hbar\omega$ excitations. However, we include mixing of n_π and this requires to test convergence for increasing N. This type of Hamiltonian was applied successfully in several studies, of which we cite here only a few [6, 7].

The semi-classical potential is obtained by choosing first a trial state $\mid \alpha\rangle$ and then calculating the expectation value of the Hamiltonian with respect to this normalized trial state, i.e., $V(\alpha) = \langle\alpha \mid \boldsymbol{H} \mid \alpha\rangle$. Here α is a short hand notation for the variables of the state.

As a trial state we use

$$\begin{aligned}
|\alpha\rangle &= \mathcal{N}_{N,n_0}(\alpha\cdot\pi^\dagger)^{n_0}\left[\sigma^\dagger + \left(\alpha\cdot\pi^\dagger\right)\right]^N|0\rangle \\
&= \mathcal{N}_{N,n_0}\frac{N!}{(N+n_0)!}\frac{\mathrm{d}^{n_0}}{\mathrm{d}\gamma_1^{n_0}}\left[\sigma^\dagger + \gamma_1\left(\alpha\cdot\pi^\dagger\right)\right]^{N+n_0}|0\rangle \ ,
\end{aligned} \tag{3}$$

where, for convenience, we redefined the total number of relative oscillator quanta as $(N + n_0)$, while the γ_1 parameter has to be set equal to 1 after the differentiation, and the normalization factor $\mathcal{N}_{N,n_0}$ is given in [8]. Already here we obtain an essential difference with respect to the case when the Pauli principle is not observed. As shown in [8], the α variable is proportional to $\sqrt{n_0}$ and also proportional to the separation of the clusters. Thus the so-called vibrational limit ($\alpha = 0$) describes already a deformed system. Nevertheless, we shall keep the notation as it is. A special limit arises when n_0 is set to zero, i.e. no Pauli exclusion principle is observed. Models with this property we call PACM (*Phenomenologic Algebraic Cluster Model*).

The resulting potential has a surprisingly simple structure. The main part depends on only three parameters and is given by

$$\tilde{V}(\alpha) = \left(A(x,y)\alpha^2 \frac{F_{11}\left(\alpha^2\right)}{F_{00}\left(\alpha^2\right)} - B(x,y)\alpha^4 \frac{F_{22}\left(\alpha^2\right)}{F_{00}\left(\alpha^2\right)} + \alpha^6 \frac{F_{33}\left(\alpha^2\right)}{F_{00}\left(\alpha^2\right)} - C(x,y)\alpha^2 \frac{F_{20}\left(\alpha^2\right)}{F_{00}\left(\alpha^2\right)} \right). \quad (4)$$

The expressions for $F_{pq}\left(\alpha^2\right)$ as well as for the coefficients $A\left(x,y\right)$, $B\left(x,y\right)$ and $C\left(x,y\right)$ can be found in Ref. [9]. They are functions of all parameters of the model. *It is important to note that although the Hamiltonians depends on many parameters, the semi-classical potential depends effectively only on three of them. Thus the discussion of phase transition properties is reduced to the variation of three parameters only!* The same potential could, in principle, be obtained in the PACM too, by paying the price of the introduction of non-polynomial interactions. This is similar to simulating Fermi repulsion in nucleus-nucleus collisions with a potential that is repulsive for small distances.

Phase transition is investigated, following the steps: i) The minima of the potential are determined numerically. There will appear only two possible minima, a deformed ($\alpha_2 > 0$) and a spherical one, the latter corresponding to $\alpha_1 = 0$. The point $\alpha_1 = 0$ is always an extremum. ii) The three parameters are varied and those points are determined, where the two minima coincide. These points, which form a surface in the space of the parameters, are at the phase transition boundary. iii) The corresponding α variables are substituted into the potential. For the spherical minimum $\alpha_1 = 0$ is always zero, which results in an expression for the potential which is *identical zero*, and therefore the derivatives of it with respect to the parameters is always zero. iv) The derivatives with respect to the parameters are determined and compared at the point of phase transition. Due to the structure of the potential a simple rule could be derived [9, 10]: If α_2 at the point of phase transition is greater than zero, then the first derivatives in the two potential minima are different and the transition is, therefore, of first-order. However, when α_2 tends to zero approaching the point of phase transition, then the phase transition is of second order. The new feature is that from a given point on, no phase transition appears and a critical line is obtained. As a conclusion, the SACM permits first- and second-order phase transitions. The situation is illustrated in fig. 1. In the right panel α_2 is plotted versus A and C (B is determined via the condition that only points at the surface of phase transition are considered). The area where α_2 is zero represents the surface of second-order phase transition, while the other area corresponds to the surface of a first-order phase transition. In the left panel this surface is plotted in the space of the parameters. Note the appearance of a dashed line (the solid line separates the first- from the second-order phase transitions). Beyond this line no phase transition appears and this represents a critical line.

The same considerations were applied, i.e. in the PACM, where the minimal number of π-oscillation quanta is zero. Though the Hamiltonian is the same, the semi-classical potential changes significantly. The important part has the form

$$\tilde{V}\left(\beta\right) \;=\; \left\{ A\beta^2 - B\beta^4 + \beta^6 \right\} \quad , \quad (5)$$

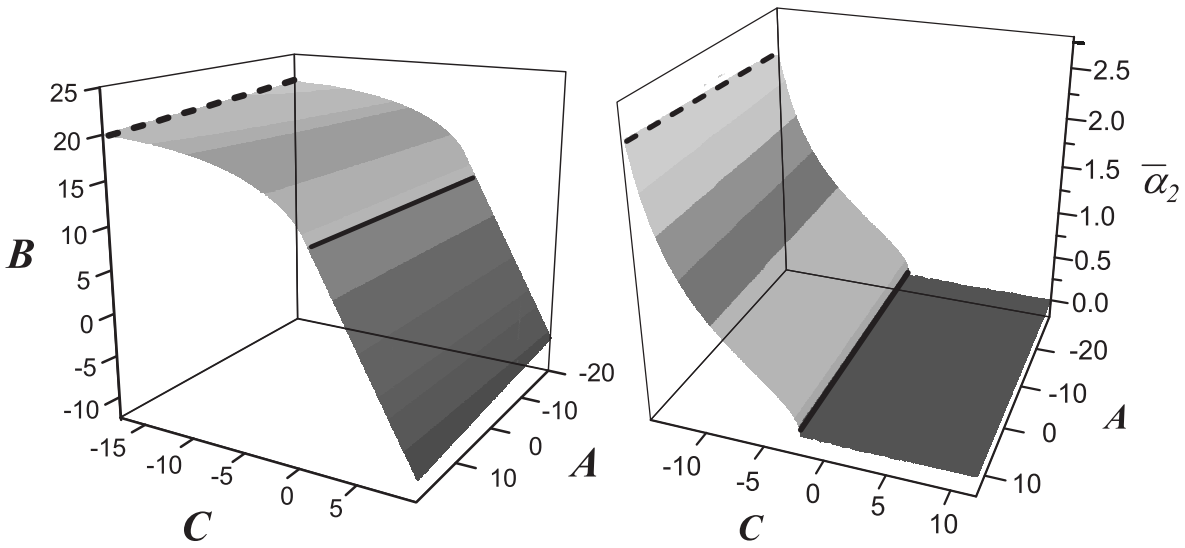

Figure 1. The phase space diagram of the SACM as a function of the independent parameters A, B and C (left panel) . The solid line marks the change from a second- to a first-order phase transition, the dashed line indicates a *critical line*. The variable $\bar{\alpha}_2$ of the deformed solution, as a function in A and C. B is fixed by the requirement that one is at a point of a phase transition (right panel).

with $\beta^2 = \frac{\alpha^2}{1+\alpha^2}$. The expression for the coefficients $A\,(x, y)$ and $B\,(x, y)$, can be found in Ref. [9]. The points of phase transitions now form a line. First- and second-order phase transition appear but not a critical point. The first-order phase transition appears due to the inclusion of a third-order interaction in the $SU(3)$ Hamiltonian, otherwise only second-order phase transitions are permitted.

In fig. 2 the space of phase transitions is plotted. There are only two relevant parameters A

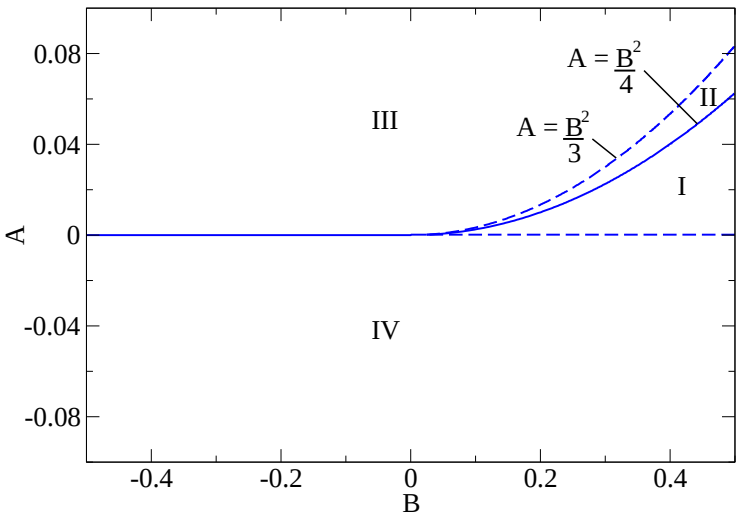

Figure 2. The parameter phase diagram for the PACM. The horizontal axis is B, while the vertical axis corresponds to A. In Region I and Region II two minima exist, one spherical and one deformed. In Region I the global minimum is the deformed one, while in Region II it is the spherical minimum. In Region III only a spherical minimum exists and in Region IV the only minimum is a deformed one.

Finally, we would like to point out severe problems for states at low energy, when the Pauli exclusion principle is not observed. As an example we consider the ^{16}O+$\alpha \rightarrow {}^{20}$Ne system. In

the $SU(3)$ limit the ground state would be formed by a 0^+ state in the (0,0) $SU(3)$-irrep, a 2^+ state in (2,0), a 4^+ state in (4,0), etc. Even when one adds the interaction term $\boldsymbol{L}^2$, which gives a rotational $L(L+1)$ structure, simulating a rotational band, this band is not rotational because each state has a different intrinsic structure. Using the $SO(4)$ dynamical symmetry limit gives a quite good agreement to experiment (!), however, the resulting states jump between low n_π and hight n_π, near the cut-off N, making the result dubious. Another problem appears in the geometrical limit: the interaction $\left[\left(\hat{\pi}^\dagger\cdot\hat{\pi}^\dagger\right)-\left(\sigma^\dagger\right)^2\right]\left[(\hat{\pi}\cdot\hat{\pi})-(\hat{\sigma})^2\right]$ tends to a potential of the type $\left[af(\alpha)\alpha^2-bN\right]$, where $f(\alpha)$ is a simple expression of the order of one and a, b depend on N and n_0 (which is 0 for the PACM and >0 for the SACM). Removing the cut-off ($N\to\infty$) the minimum of the deformed potential tends to infinity too, being more equivalent to a dissociation limit. This problem arises in both the SACM and PACM, shedding doubt on the physical meaning of the $SO(4)$ dynamical symmetry as a deformed limit.

3. Conclusions

In this contribution we showed that the SACM permits a very rich structure of phase transitions, including first and second order. A critical line also appears. When the Pauli exclusion principle is not observed, and a Hamiltonian of up to third order interactions is applied, then first- and second-order phase transitions still appear, but not a critical line. The results of the SACM could, in principle, be also reproduced within the PACM, but only paying the price of using a very complicated non-polynomial interaction that simulates the Pauli-exclusion principle. We also showed that neglecting the Pauli exclusion principle leads to dubious behavior for the states at low energy, even though the experimental spectrum is well reproduced. This puts some doubt on the argument that when the experiment is reproduced the model is fine. More has to be included, such as the structure of the states and the fulfillment of basic principles, as the Pauli exclusion principle is. These deficiencies may, of course, manifest themselves in failing to reproduce further experimental observables not discussed in the model.

Finally, we discussed the physical interpretation of the $SO(4)$ dynamical symmetry limit, which rather describes a dissociation of the cluster system than a deformed limit.

Acknowledgments

We gratefully acknowledge financial help from DGAPA-PAPIIT (no. IN103212), DGAPA, from the National Research Council of Mexico (CONACyT), OTKA (grant No. K72357), and from the MTA-CONACyT joint project. P.O.H. thanks the Frankfurt Institute for Advances Studies (FIAS) and the GSI for excellent working atmosphere and all the help received.

References

[1] Cseh J 1992 *Phys. Lett.* B **281** 173
[2] Cseh J and Lévai G 1994 *Ann. Phys. (N.Y.)* **230** 165
[3] Elliott J P 1958 *Proc. Roy. Soc.* A **245** 128
Elliott J P 1958 *Proc. Roy. Soc.* A **245** 562
[4] Darai J, Cseh J and Jenkins D G 2012 *Phys. Rev.* C **86** 064309
[5] Sciani W, Otani Y, Lépine-Szily A, Benjamim E A, Chamon L C, Lichtenthäler Filho R, Darai J and Cseh J 2009 *Phys. Rev.* C **80** 034319
Cseh J, Darai J, Sciani W, Otani Y, Lépine-Szily A, Benjamim E A, Chamon L C and Lichtenthäler Filho R 2009 *Phys. Rev.* C **80** 034320
[6] Cseh J and Darai J 2006 *Acta Univ. Debrecen, Ser. Phys. Chim.* **XL** 23
[7] Cseh J and Darai J 2008 *AIP Conf. Proc.* (Fusion08) **1098** 225
[8] Hess P O, Lévai G and Cseh J 1996 *Phys. Rev.* C **54** 2345
[9] Yépez-Martínez H, Fraser P R, Hess P O and Lévai G 2012 *Phys. Rev.* C **85** 014316
[10] Fraser P R, Yépez-Martínez H, Hess P O and Lévai G 2012 *Phys. Rev.* C **85** 014317